AD-A172 825 HOLOGRAPHIC PROPERTIES OF DMP-128 PHOTOPOLYMERS(U) DUKE 1/1
UNIV DURHAM NC B D GUENTHER ET AL. 05 SEP 86
ARO-23204.1-PH DAAL03-86-C-0005

UNCLASSIFIED F/G 14/5 NL

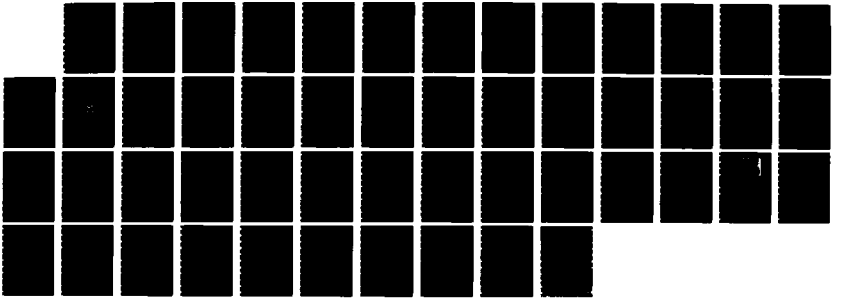

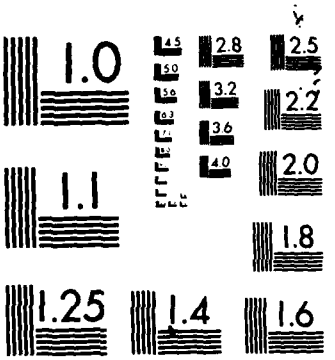

MICROCOPY RESOLUTION TEST CHART
NATIONAL BUREAU OF STANDARDS-1963-A

ARO-23204.1-PH

TITLE

HOLOGRAPHIC PROPERTIES OF DMP-128 PHOTOPOLYMERS

TYPE OF REPORT (TECHNICAL, FINAL, ETC.)

FINAL

AUTHOR (S)

B. D. Guenther and William Hay

DATE

9/5/86

U. S. ARMY RESEARCH OFFICE

CONTRACT/ GRANT NUMBER

DAAL03-86-C-0005

INSTITUTION

DUKE UNIVERSITY

86-10-8-118

UNCLASSIFIED
SECURITY CLASSIFICATION OF THIS PAGE

REPORT DOCUMENTATION PAGE

1a. REPORT SECURITY CLASSIFICATION Unclassified	1b. RESTRICTIVE MARKINGS
2a. SECURITY CLASSIFICATION AUTHORITY	3. DISTRIBUTION/AVAILABILITY OF REPORT Approved for public release; distribution unlimited.
2b. DECLASSIFICATION/DOWNGRADING SCHEDULE	
4. PERFORMING ORGANIZATION REPORT NUMBER(S)	5. MONITORING ORGANIZATION REPORT NUMBER(S) ARO 23204.1-PH
6a. NAME OF PERFORMING ORGANIZATION DUKE UNIVERSITY 6b. OFFICE SYMBOL (If applicable)	7a. NAME OF MONITORING ORGANIZATION U. S. Army Research Office
6c. ADDRESS (City, State, and ZIP Code) DURHAM, NC	7b. ADDRESS (City, State, and ZIP Code) P. O. Box 12211 Research Triangle Park, NC 27709-2211
8a. NAME OF FUNDING/SPONSORING ORGANIZATION U. S. Army Research Office 8b. OFFICE SYMBOL (If applicable)	9. PROCUREMENT INSTRUMENT IDENTIFICATION NUMBER DAAL03-86-C-0005
8c. ADDRESS (City, State, and ZIP Code) P. O. Box 12211 Research Triangle Park, NC 27709-2211	10. SOURCE OF FUNDING NUMBERS PROGRAM ELEMENT NO. / PROJECT NO. / TASK NO. / WORK UNIT ACCESSION NO.

11. TITLE (Include Security Classification)

HOLOGRAPHIC PROPERTIES OF DMP-128 PHOTOPOLYMERS

12. PERSONAL AUTHOR(S)

B. D. Guenther and William Hay

13a. TYPE OF REPORT	13b. TIME COVERED	14. DATE OF REPORT (Year, Month, Day)	15. PAGE COUNT
Final	FROM 11/15/85 TO 12/31/86	September 5, 1986	42

16. SUPPLEMENTARY NOTATION

The view, opinions and/or findings contained in this report are those of the author(s) and should not be construed as an official Department of the Army position, policy, or decision, unless so designated by other documentation.

17. COSATI CODES			18. SUBJECT TERMS (Continue on reverse if necessary and identify by block number)
FIELD	GROUP	SUB-GROUP	

19. ABSTRACT (Continue on reverse if necessary and identify by block number)

The holographic properties of the photopolymer DMP-128 produced by Polaroid were measured. Holograms with a diffraction efficiency of 90% and index modulation in excess of 0.06 was achieved. Both surface relief and volume phase modulation were observed to be present. Wavelengths and angular sensitivity were measured. Handling and processing properties were discussed.

20. DISTRIBUTION/AVAILABILITY OF ABSTRACT ☐ UNCLASSIFIED/UNLIMITED ☐ SAME AS RPT. ☐ DTIC USERS	21. ABSTRACT SECURITY CLASSIFICATION Unclassified
22a. NAME OF RESPONSIBLE INDIVIDUAL	22b. TELEPHONE (Include Area Code) / 22c. OFFICE SYMBOL

CONTENTS

LIST OF FIGURES

Chapter 1. INTRODUCTION

Ever since Denis Gabor discovered the principles of wavefront reconstruction (or holography) in 1948, efforts have been made to improve the quality of the reconstructed holographic image. In the early 60's, Leith and Uptanieks improved the performance of holography by using separate object and reference beams [1]. The invention of the laser shortly thereafter spurred increased research activity in holography as more powerful coherent sources made quality images practicable. As in most developing technologies, a major field of continuing interest is the search for better materials. This thesis is dedicated to the characterization of a promising new development in holographic recording materials: Polaroid's DMP-128 holographic recording system.

Several material systems are suitable for the recording of holograms, but there are significant differences in the performance achieved by each. These differences pervade every aspect of the material: storage, preparation for exposure, exposure, processing and subsequent usability. Important factors which must be known before the desired hologram can be made include film sensitivity (analogous to speed in photographic film), linearity of the response to light, maximum diffraction efficiency, signal-to-noise ratio, wavelength and angular sensitivity and resolution of the film. Each of these parameters vary from material to material and can also vary with the thickness or processing of one material. Some of the presently used materials include silver halide film, dichromated gelatin, photopolymers, thermoplastics and photoresists [2]. Each of these has its advantages and disadvantages. Dichromated gelatin, the present industry standard, is capable of very high diffraction efficiency, but great care must be exercised in processing and developing the hologram. DMP-128 photopolymer exhibits some very desirable qualities, including long shelf storage time, high efficiency and ease of processing.

Chapter 2 of this thesis will include a review of the principles of holography and theory of characterization of holograms. The experimental set-up and scope of the experiments along with

the results and analysis comprise Chapter 3. Conclusions and suggestions for further research are reviewed in Chapter 4.

Chapter 2. THEORY

Holography is the science (and art) of recording the phase and intensity information in a light signal by means of interfering the signal with another, coherent beam and storing the resulting interference pattern (a concept very similar to that of modulating an electrical carrier frequency with a signal frequency). While this work is concerned mainly with one material used to record this information--Polaroid's DMP-128, a brief review of the principles of holography is in order before proceeding. This review will be constrained to signal and reference beams consisting of coherent plane or spherical waves. A description of the DMP-128 holographic recording system will follow, along with an enumeration of material concerns and parameters.

2.1 Holographic Theory

2.1.1 Interference

For a monochromatic wave of frequency *f*, the electric field $\vec{v}$ can be expressed as

$$\vec{v} = \tilde{a}\cos(2\pi ft + \phi), \tag{2.1}$$

where $\tilde{a}$ is the amplitude of oscillation and ϕ is the phase [3]. The phase ϕ contains the spatial dependence of the wave. When two or more sinusoidal waves are summed, the resulting wave is also sinusoidal, yielding

$$\tilde{a}_1\cos(2\pi ft + \phi_1) + \tilde{a}_2\cos(2\pi ft + \phi_2) + \cdots = \tilde{a}\cos(2\pi ft + \phi), \tag{2.2}$$

or in complex notation,

$$\mathrm{Re}[\tilde{a}_i\exp[i(2\pi ft + \phi_1)]] + \mathrm{Re}[\tilde{a}_2\exp[i(2\pi ft + \phi_2)]] + \cdots \tag{2.3}$$

$$= \mathrm{Re}[\tilde{a}\exp[i(2\pi ft + \phi)]].$$

The latter form is advantageous for most mathematical manipulation and shall be used here,

adopting the common convention of dropping the "Re[ ]" while still assuming its existence. As the frequency will always be held constant in this work and relative, not absolute, phase is the important factor, the temporal phase term $\exp(i2\pi ft)$ will be dropped, leaving

$$\vec{a}_1 \exp(i\phi_1) + \vec{a}_2 \exp(i\phi_2) + \cdots = \vec{a}\exp(i\phi) = \vec{a}, \tag{2.4}$$

where $\vec{a}$ is the complex vector amplitude. Complex quantities will be denoted by bold-face type.

The intensity I_p of a wave is defined as the time average of the energy flow per unit time per unit cross-sectional area,

$$I_p = 1/2s\epsilon\langle\vec{v}\cdot\vec{v}\rangle, \tag{2.5}$$

where s is the speed of light in the medium and ϵ is the dielectric constant. In holography, the intensity I is alternately defined as

$$I = 2\langle\vec{v}\cdot\vec{v}\rangle, \tag{2.6}$$

which is the square of the amplitude of the wave, or

$$I = \vec{a}\cdot\vec{a} = \vec{a}\cdot\vec{a}^{*}. \tag{2.7}$$

For the purposes of holography, we are generally concerned with only two waves--a reference and an object wave. In this case, Eq. 2.7 becomes

$$I = \vec{a}\cdot\vec{a} = \vec{a}_1\cdot\vec{a}_1 + \vec{a}_2\cdot\vec{a}_2 + 2\vec{a}_1\cdot\vec{a}_2\cos(\phi_2-\phi_1) \tag{2.8}$$

$$= I_1 + I_2 + 2(\vec{a}_1\cdot\vec{a}_2\cos(\phi_2-\phi_1)).$$

In our experimental set-up, both waves are polarized parallel to one another; the dot product reduces to scalar multiplication of the amplitudes in this case and shall be written in that form.

In the special case of forming diffraction gratings, both of these waves are plane waves.

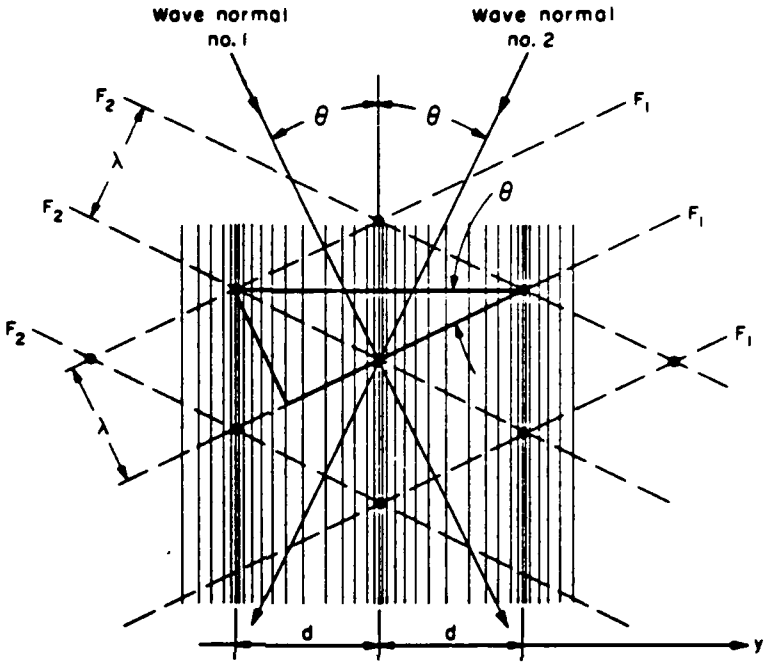

Figure 2-1. Interference pattern of two intersecting plane waves.

This is presented graphically in figure 2-1. The wavefront crests, separated by the wavelength λ, are represented by F_1 and F_2 for wave number 1 and wave number 2, respectively. Where these two wavefronts intersect, they interfere constructively, resulting in planes of the highest intensity, depicted by the close spacing of the vertical lines, which bisect the incoming wave normals. These planes lie perpendicular to the plane of the paper. It is this variance in intensity which is recorded by the hologram. The relative intensity of the two beams is known as the K-ratio, where

$$K = I_1 / I_2. \tag{2.9}$$

The importance of K can be seen by considering the maximum and minimum intensities of the

interference pattern. From Eq. 2.8 it can be seen that when K = 1 (corresponding to $I_1 = I_2$), the intensity of the fringes varies from zero to 4I. For $K \neq 1$ (corresponding to $I_1 \neq I_2$), the intensity neither falls to zero nor rises to twice that of the total incident intensity. The fringe visibility V is a measure of this fringe contrast and is defined as

$$V = \frac{I_{max} - I_{min}}{I_{max} + I_{min}} = \frac{2\sqrt{K}}{K + 1} . \tag{2.10}$$

2.1.2 Hologram formation

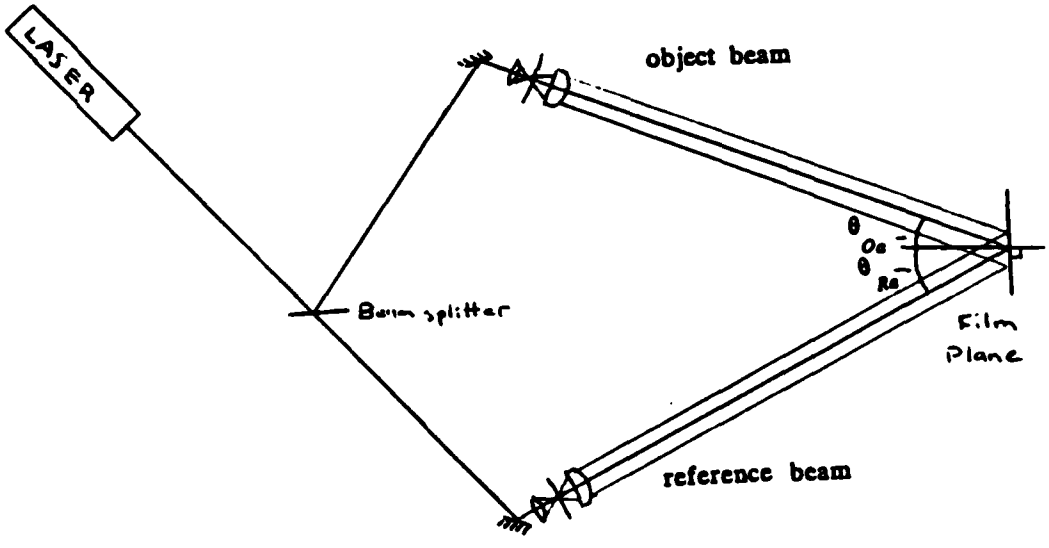

Figure 2-2. Typical geometry for forming gratings.

A typical set-up for forming diffraction gratings is shown in figure 2-2. The film will be assumed to be in the x-y plane with the z-axis as the normal to the surface; beams are assumed

to propagate in the y-z plane. The laser is split into two beams which are then spatially filtered with a microscope objective and pinhole. Next both beams are collimated and directed onto the recording medium. The reference and object beams intersect the film plane at angles θ_{Ra} and θ_{Oa}, respectively, as measured from the normal. Depending on the thickness T of the material and the angles of incidence, the resulting hologram is classified as either a plane (thin) or volume (thick) hologram. The difference and the consequences will be explained later.

Inside the medium the interfering beams produce planes of periodically varying intensity

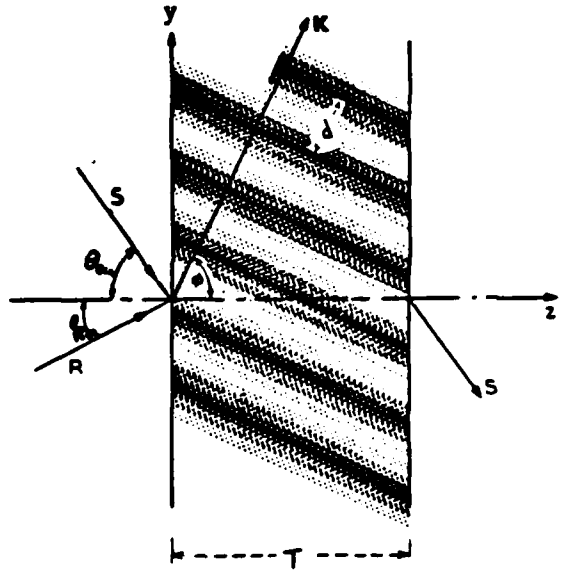

Figure 2-3. Geometry of plane wave interference in a recording medium.

which extend parallel to the x-axis. The resulting geometry is shown in figure 2-3 [4]. Upon entering the medium, the reference and object beams are refracted according to Snell's law and propagate through the medium at angles θ_R and θ_O defined by

$$\frac{\sin\theta_{Ra}}{\sin\theta_{R}} = \frac{\sin\theta_{Oa}}{\sin\theta_{O}} = n, \tag{2.11}$$

The resulting amplitude inside the medium is

$$a = a_R \exp[-i2\pi/\lambda(\sin\theta_R y + \cos\theta_R z)] + a_O \exp[-i2\pi/\lambda(\sin\theta_O y + \cos\theta_O z)], \tag{2.12}$$

and the intensity from Eq. 2.8 becomes

$$I = I_R + I_O + 2(I_R I_O)^{1/2} \cos[2\pi/\lambda[(\sin\theta_O - \sin\theta_R)y + (\cos\theta_O - \cos\theta_R)z]], \tag{2.13}$$

where I_R and I_O are the intensities of the reference and object beams. At the air-medium interface, the fringe spacing in the y-direction d_y is

$$d_y = \frac{\lambda}{\sin\theta_O - \sin\theta_R}, \tag{2.14}$$

obtained by setting $z=0$ and solving for adjacent intensity maxima. The fringe planes bisect θ_R and θ_O and the angle they make with medium boundary, called the slant angle ϕ, is

$$\phi = \frac{\pi}{2} - \frac{\theta_R + \theta_O}{2}. \tag{2.15}$$

The distance between the crests is called the fringe period d and is equal to

$$d = d_y \sin\phi. \tag{2.16}$$

The grating vector $\bar{K}$ is perpendicular to the fringe planes and has the value

$$K = 2\pi / d. \tag{2.17}$$

In order to record the interference pattern described above, the medium must respond in some way to the intensity of the light. This can be done either by changing the real transmittance, the thickness, or the index of refraction of the medium [3]. The first type is known as absorption hologram, while the latter two are known as phase holograms. Also known as surface relief, the thickness variation changes the phase by controlling the distance the beam propagates in the medium; the phase is retarded for rays which travel farther in the material, because the higher index of refraction creates a longer optical path length. In the last case, the incoming rays are diffracted by the changing index of refraction in the medium. All three effects may be present in any hologram, but one type usually predominates. DMP-128 changes index of refraction with exposure and records the fringes as a spatial modulation of the index of refraction, $n = n_0 + n_m(y,z)$. In addition to the change of index of refraction, there may be some surface relief involved due to mass transport and changes in density.

2.1.3 Hologram reconstruction

A hologram is considered to be a volume hologram if light diffracted by it during reconstruction passes through several fringe planes [2]. If a hologram is too thin or the fringes are spread too far apart, the diffracted beam interacts with only one or two fringes and the hologram is essentially a planar construction. The parameter Q is used to distinguish between volume and plane holograms [4], where

$$Q = 2\pi\lambda_a T/nd^2. \tag{2.18}$$

While the transition between volume and plane holograms is somewhat gradual, it is generally accepted that for $Q \geq 10$, the holographic properties are based on volume diffraction.

2.1.3.1 Plane holography In the case of a thin hologram, Eq. 2.13 reduces to

$$I = I_O + I_R + 2(I_O I_R)^{(1/2)} \cos[2\pi/\lambda(\sin\theta_O - \sin\theta_R)y], \tag{2.19}$$

as the hologram is negligibly thin in the z direction. The recording medium is modulated proportionately to the intensity I(y), causing a phase shift $\phi(y)$ on a plane wave propagating through the developed hologram [1], expressed by

$$\phi(y) \propto I(y) \tag{2.20}$$

$$= I_O + I_R + 2(I_O I_R)^{(1/2)} \cos[2\pi/\lambda(\sin\theta_O - \sin\theta_R)y]$$

$$= \phi_0 + \phi_1 \cos[2\pi/\lambda(\sin\theta_O - \sin\theta_R)y].$$

The light passing through the developed hologram relative to the light incident on it is called the transmittance. In the case of a lossless phase hologram, the transmittance is a complex number of unit value. Thus the transmittance t of a thin hologram is

$$t = \exp(i\phi_0)\exp[i\phi_1 \cos[(2\pi/\lambda)(\sin\theta_O - \sin\theta_R)y]. \tag{2.21}$$

Neglecting the constant phase factor which has no imaging effect, we can express the transmittance as a Fourier series

$$t = \sum_{n=-\infty}^{+\infty} i^n J_n(\phi_1)\exp[(in2\pi/\lambda)(\sin\theta_O - \sin\theta_R)y], \tag{2.22}$$

where J_n is a Bessel function of the first kind and *nth* order. Each of the summed terms corresponds to a diffracted order of the signal beam [5]. The first diffracted order is represented by the term for n = 1:

$$t_1 = iJ_1(\phi_1)\exp[(i2\pi/\lambda)(\sin\theta_O - \sin\theta_R)y], \tag{2.23}$$

of which the amplitude is simply $J_1(\phi_1)$. For a reference beam of unit amplitude, the maximum amplitude of the first order Bessel function is .582, thus the maximum diffraction efficiency for

thin phase holograms is $a^2 = .582^2$ or 33.9%. This relatively low maximum diffraction efficiency would be severely limiting to practical applications of holography where high efficiency is required, but as is shown in the next section, higher efficiencies are obtainable in volume holograms.

2.1.3.2 Volume holography In efficient volume holograms one must consider the attenuation of the reference beam when analyzing diffraction. Kogelnik adapted coupled wave theory analysis to holographic volume diffraction gratings in order to account for the high diffraction efficiencies obtainable [4]. His analysis is followed here.

A wave propagates in the medium according to the wave equation

$$\nabla^2 a + k^2 a = 0, \tag{2.24}$$

where k is the propagation constant defined by

$$k = 2\pi n / \lambda_a, \tag{2.25}$$

assuming a lossless medium. The index of refraction is assumed to vary sinusoidally with an average value n_0 and an index of modulation n_1, or

$$n = n_0 + n_1 \cos(\vec{K}\cdot\hat{y}). \tag{2.26}$$

where $\hat{y}$ is a unit vector in the y-direction. The incident reference wave a_R can be written as

$$a_R = R(z)\exp(-i\vec{\rho}\cdot\hat{y}), \tag{2.27}$$

where $\vec{\rho}$ is the direction of wave propagation. Similarly the amplitude of the diffracted signal wave a_S is

$$a_S = S(z)\exp(-i\vec{\sigma}\cdot\hat{y}), \tag{2.28}$$

where $\vec{\sigma}$ is the direction of propagation of the diffracted wave. $\vec{\rho}$ and $\vec{\sigma}$ and their relationship to

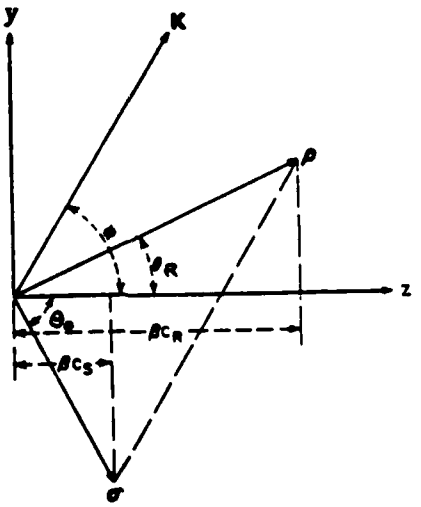

Figure 2-4. The propagation vectors $\vec{\rho}$ and $\vec{\sigma}$ of the reference and signal waves and their relationship to the grating vector $\vec{K}$. Their respective obliquity factors are also shown.

$\vec{K}$ are depicted in figure 2-4. These waves are coupled by a transfer of energy between them. The amplitude of the total electric field is thus

$$a = a_R + a_S = R(z)\exp(-i\vec{\rho}\cdot\hat{\gamma}) + S(z)\exp(-i\vec{\sigma}\cdot\hat{\gamma}). \tag{2.29}$$

If θ differs from the Bragg angle θ_0 by $\Delta\theta$ or the reference wavelength differs from the recording wavelength by $\Delta\lambda$, the Bragg condition is not met and a "detuning" or "dephasing" occurs. The dephasing measure δ is defined as

$$\delta = \Delta\theta\, K\sin(\theta_0 - \phi) - \Delta\lambda\, K^2 / 4\pi n. \tag{2.30}$$

The obliquity factors c_R and c_S are related to the propagation of the reference and signal waves in the z direction, respectively, and are given by

$$c_R = \cos\theta \tag{2.31a}$$

$$c_S = \cos\theta - \frac{\lambda}{n_0 d}\cos\phi. \tag{2.31b}$$

They are shown in figure 2-4, using $\beta = 2\pi n/\lambda$.

When the coupled wave equation is solved for the case of phase transmission gratings--$R(z=0)=1$, $S(z=0)=0$--we obtain the amplitude of the emerging signal wave

$$S(T) = -i(c_R/c_S)^{(1/2)} \exp(-i\xi)\sin(\nu^2 + \xi^2)^{(1/2)}/(1 + \xi^2/\nu^2)^{(1/2)}, \tag{2.32}$$

where

$$\nu = \pi n_1 T/\lambda_a (c_R c_S)^{(1/2)} \tag{2.33}$$

and

$$\xi = \delta T/2c_S. \tag{2.34}$$

The diffraction efficiency η is defined as the fraction of incident power diffracted into the signal wave, which is written as

$$\eta = (|c_S|/c_R)SS^*. \tag{2.35}$$

This can now be calculated to be

$$\eta = \sin^2(\nu^2 + \xi^2)^{(1/2)}/(1 + \xi^2/\nu^2). \tag{2.36}$$

In the case when the fringe planes are perpendicular to the medium boundaries ($\phi = \pi/2$), this reduces to:

$$\eta = \sin^2(\pi n_1 T/\lambda\cos\theta_0). \tag{2.37}$$

From Eq. 2.37 it can be seen that the theoretical maximum diffraction efficiency of volume phase holograms is 100% for $\pi n_1 T/\lambda\cos\theta_0 = (2x + 1)\pi/2$, for any integer x.

Also of interest are the angular and wavelength sensitivities of a hologram. When $\Delta\lambda = 0$, the angular deviation can be expressed as

$$\xi = \Delta\theta K d\sin(\phi - \theta_0)/2c_{s.} \tag{2.38}$$

Similarly, for $\Delta\theta = 0$, the wavelength deviation can be expressed as

$$\xi = \Delta\lambda K^2 d/8\pi nC_{s.} \tag{2.39}$$

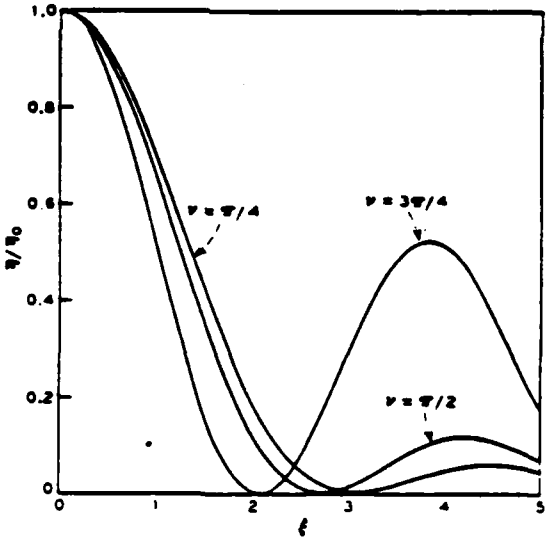

Figure 2-5. η/η_0 vs. ξ--angular and wavelength sensitivity of lossless phase gratings.

The sensitivities can be shown as a function of ν as in figure 2.5, where η/η_0 is the normalized diffraction efficiency. For increasing values of ν, the sensitivity curve narrows and side lobes

become much larger. Increasing ν can correspond to increasing index of modulation, thickness or incident construction angle. For unslanted gratings, the half-power bandwidths can be approximated by

$$2\Delta\theta_{(1/2)} \approx d/T \tag{2.40a}$$

and

$$2\Delta\lambda_{(1/2)} \approx \cot(\theta)d/T. \tag{2.40b}$$

These bandwidth calculations are only approximate as Kogelnik's theory assumes that $\Delta\theta \ll 1$ in order to solve the wave equation (Eq. 2.24) for the coupled signal and reference waves.

2.2 The Material

The Polaroid DMP-128 holographic film is a photopolymer system which produces phase holograms. Photopolymer systems for holography were first developed in the late 1960's by Hughes Aircraft [6]. Another notable commercial development of a similar system was by Booth at Dupont.

A typical photopolymer system consists of a polymer (often called the binder), a monomer (or monomers) and a dye [6]. The polymer adds physical strength to the emulsion and aids in the coating of the emulsion substrate. The dye absorbs the incident light, thereby providing the initiation energy for the photochemical reactions which lead to the polymerization of the monomer. One photon can provide enough energy to form a molecule chain of hundreds of monomer units, accounting for the good sensitivity of the DMP-128 material [7]. The polymerized molecule has a different index of refraction from that of the monomer, resulting in a gradient in the index of refraction in the material responsible for hologram formation. The frequency range over which the Polaroid system is sensitive is determined by the absorption spectrum of the incorporated dye and can thus be altered by the selection of specific dyes.

While the exact mechanism of fringe recording in DMP-128 and other photopolymers is not known, several basic tenets are postulated. When light strikes the photopolymer, the monomers in that region join to form large chains of molecules. This depletion of the monomers in one region causes a gradient in monomer concentration. The monomers in the higher concentration regions tend to diffuse to the regions of lower concentration, where they are also polymerized. This movement of the monomers and polymerization of the material could cause thickness variations in the material which would yield a surface relief effect. The polymerization into large molecules is known to cause a change in index of refraction in the bulk material, so this effect can form volume holograms in which the index of refraction is selectively modulated. When the material is illuminated with white light after exposure, this thickness variation or index of refraction modulation is frozen by the polymerization of all the remaining monomer. Shankoff has theorized that the diffraction in dichromated gelatin is caused by miniscule cracks in the emulsion which are filled with air [8]. This is also a possibility in DMP-128.

DMP-128 is available in three formulations which contain different dyes: one is sensitive in the blue region of the spectrum, one in the green and the other in the red. In this report, the discussion will be limited to the red-sensitive film. The film is also available in varying thicknesses ranging from three to twenty microns, but this report will be confined to seven micron emulsions. The emulsion has a bulk index of refraction of 1.53 [9] and is supported on a flint glass substrate which has an index of refraction that closely matches that of the photopolymer.

2.2.1 Material parameters

A holographic recording material has several associated parameters which quantify its response to the interference pattern which forms the hologram. Among these are sensitivity, linearity and resolution. These parameters must be considered during hologram formation in order to achieve the desired results for hologram reconstruction.

The sensitivity S is a measure of the amount of change in the material as a function of exposure energy [3]. It is defined by the equation

$$\sqrt{\eta} = SE_0V, \tag{2.41}$$

where E_0 is the average exposure over the hologram. For an ideal hologram where the reconstructed wavefront is linearly proportional to the original object wave front, S is independent of V and E_0. In real recording materials, however, S is not independent and linearity is a non-quantitative measure of how S depends on V and E_o. A plot of $\sqrt{\eta}$ vs. E_0

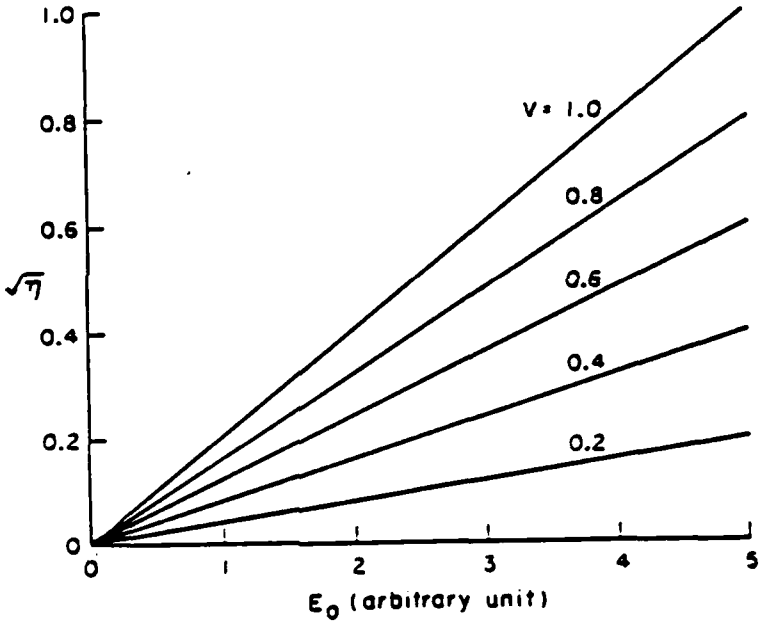

Figure 2-6. A plot of $\sqrt{\eta}$ vs. E_0 for the ideal recording material--lines of constant V are shown.

with various constant values of V is shown in figure 2-6. The characteristics of each value of V are perfectly straight, indicating linear S. The analogous plot of $\sqrt{\eta}$ vs V for constant E_0 is shown in figure 2-7.

In an ideal material, all of the incident light would be diffracted into the emerging signal

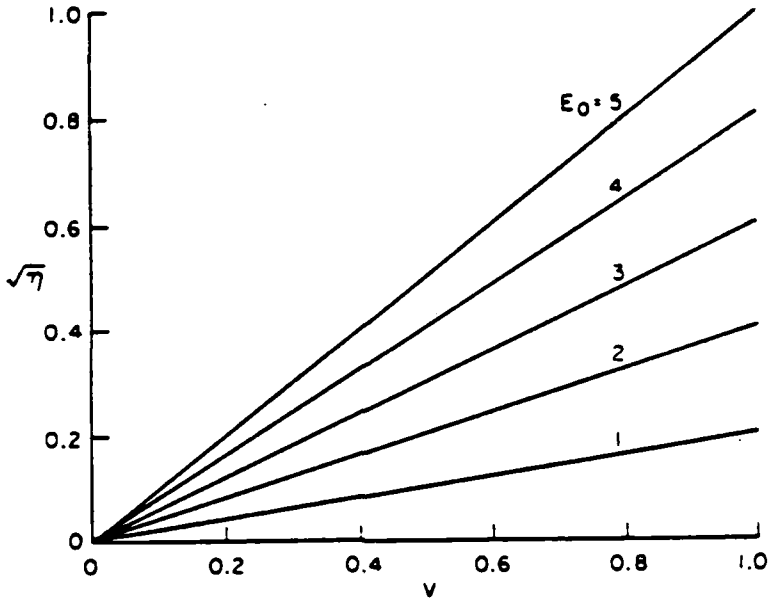

Figure 2-7. A plot of $\sqrt{\eta}$ vs. V for the ideal recording material--lines of constant E_0 are shown.

beam. Unfortunately, even with perfect holographic technique, the signal is accompanied by some noise due to imperfections in the hologram and nonlinear recording. The major film imperfection, neglecting gross macroscopic faults, is that of surface modulation. While the surface effect can itself form holograms, this causes a generally undesired phase shift in volume holograms. This effect can be minimized by use of index-matching. Nonlinearity is a more serious problem. For nonlinear S, the $\sqrt{\eta}$ vs. E_0 and V curves can be approximated by polynomial expressions. The first order term accounts for the desired linear response, but the quadratic and higher order terms cause ghost images and halos. In the case of the diffraction grating, the higher order terms diffract light into other orders much like a Fresnel zone plate or Ronchi ruling.

Recording resolution is the measure of minimum fringe spacing in the material [3]. Fringe frequency ν is the reciprocal of the period,

$$\nu = 1/d. \tag{2.42}$$

For transmission holography, the maximum frequency needed can be found by taking most extreme angles possible in the constructing geometry. Trivially, for the reference and object beams incident at the same angle, $\nu = 0$; for incident beams with the maximum interbeam angle $\theta_{Ra} = -\theta_{Oa} = \pi/2$, $\nu = 2/\lambda_a$. Letting $\lambda_a = .6328$ μm, $0 < \nu < 3160$ cycles/mm. In reflection holography, where the fringe planes are parallel to the medium surface, the fringes are separated by

$$d_z = \frac{\lambda}{2(1 - \sin^2\theta)^{(1/2)}} = \frac{\lambda_a}{2(n_o^2 - \sin^2\theta_a)^{(1/2)}}. \tag{2.43}$$

Letting $n_0 = 1.5$ and $\lambda_a = .6328$ μm while varying θ_a from $\pi/2$ to 0, we obtain $4700 < (\nu_z = 1/d_z) < 5700$ cycles/mm. If a recording medium can not support as high a resolution as is required, the image will be degraded.

2.2.2 Shrinkage of the emulsion

One difficulty inherent in many holographic media is that of swelling and shrinkage. This change in size can be quite detrimental to the accurate reconstruction of the recorded image. The activation and processing steps generally add to or deplete various constituents in the emulsion. In dichromated gelatin this can actually increase the thickness of the emulsion by three or four times at certain stages of the processing [2]. Silver halide films tend to shrink by approximately 15% of pre-exposure thickness as a result of normal development [3]. DMP-128 also exhibits a certain degree of thickness variability as a function of processing.

In general there is little lateral shrinkage in a hologram, as the emulsion is stretched out on a rigid substrate which prevents this. Excessive lateral shrinkage or swelling would result in the

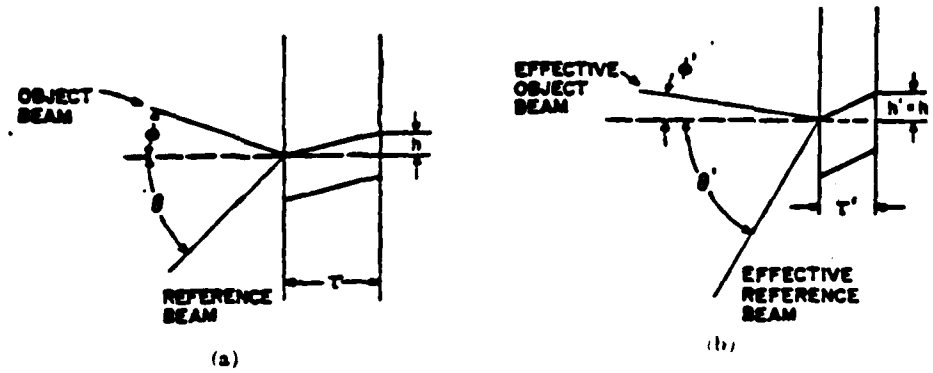

Figure 2-8. Geometry of shrinkage. (a) Before. (b) After.

tearing or folding of the emulsion and the probable destruction of the hologram. As shown in figure 2-8, the major effect of shrinkage is the tilting of the fringe planes [10]. The fringe spacing in the y-direction d_y remains constant due to lack of lateral shrinkage, but the change in thickness results in a change in the slant angle along with the grating period. Consequently, the Bragg angle changes and the hologram does not reconstruct exactly. In effect, the hologram acts as if it had been formed using different construction angles, symmetric around the new fringe planes. While the original slant angle was

$$\phi = (\theta_O - \theta_R) / 2 = \arctan(h / T), \tag{2.44}$$

the new slant angle ϕ' is

$$\phi' = (\theta'_O - \theta'_R) / 2 = \arctan(h / T'), \tag{2.45}$$

Also, retaining the fringe spacing along the y-axis,

$$\frac{\lambda}{(\sin\theta_O + \sin\theta_R)} = \frac{\lambda}{(\sin\theta'_O + \sin\theta'_R)}. \tag{2.46}$$

Solved simultaneously, these equations become

$$\sin\theta_O + \sin\theta_R = \sin\theta'_O + \sin\theta'_R \tag{2.47}$$

and

$$\frac{\theta_O - \theta_R}{2} = \frac{\theta'_O - \theta'_R}{2} \frac{\arctan(h/T)}{\arctan(h/sT)}, \tag{2.48}$$

where $s = T'/T$. For small angles, where $\sin x \approx \tan x \approx x$, Eqs. 2.48 become

$$(1/s)(\theta_O - \theta_R) = \theta'_O - \theta'_R \tag{2.49a}$$

$$\theta_O + \theta_R = \theta'_O + \theta'_R . \tag{2.49b}$$

Chapter 3. EXPERIMENT AND ANALYSIS

This chapter will describe the experimental set-up and methods used in making holograms with DMP-128. The data and results will then be presented and discussed according to the theory presented in Chapter 2.

3.1 The Experimental Set-up

Holograms were formed using the Leith-Uptanieks geometry described in Chapter 2 and

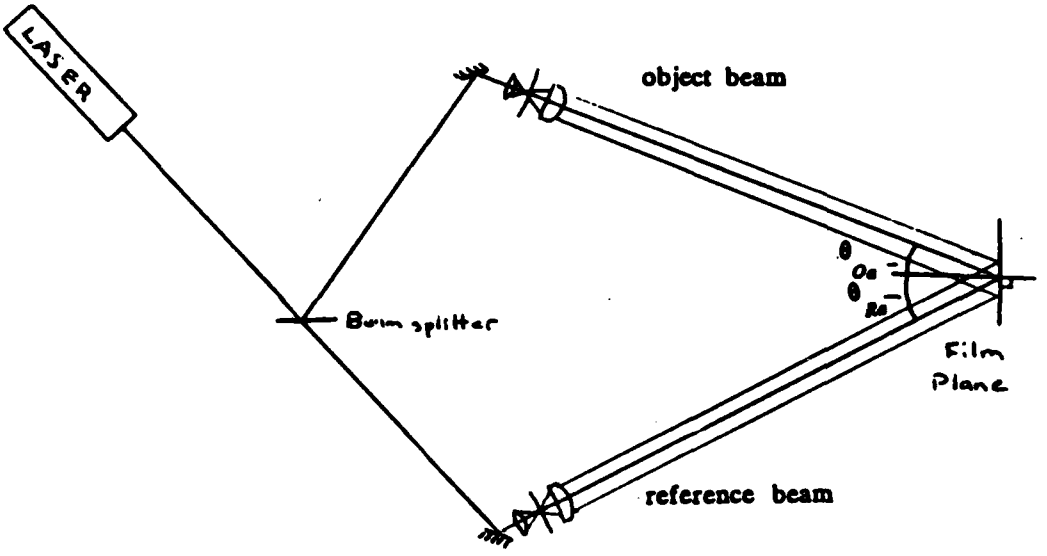

Figure 3-1. Experimental set-up to form diffraction gratings

shown here in figure 3-1. The beam from the He-Ne laser (λ_a = 632.8 nm) is split using a variable beam-splitter and then spatially-filtered using 10x microscope objectives and 25 μm pinholes. This removes any incoherent elements in the laser light. The beams are collimated and directed onto the film, intersecting the film plane normal at angles of θ_{Ra} and θ_{Oa} for the reference and object beams, respectively. Holographic lenses (gratings with focusing power) are formed by eliminating the collimating lens in the object beam path, leaving a spherically diverging wave as the object beam.

During exposure, the film is secured in a film holder adapted from Polaroid consisting of a prism with a trough secured on the front face. The trough is filled with xylene (index of refraction = 1.494) which holds the coated substrate against the prism by capillary action. In order to prevent reflection at interfaces where the index of refraction changes abruptly (which would cause additional interference in the material and result in a destructive "wood-grain" pattern), the xylene, the substrate and the prism were all chosen with $n \approx 1.5$ in order to match the index of refraction of the emulsion. The prism is also used instead of a glass plate to prevent reflection from parallel surfaces back through the emulsion.

The variables of exposure were the angles of incidence, the visibility and the exposure time (hence exposure energy). Pains were taken to keep all other variables such as activation, flooding time and chemical processing as constant as possible. The film used during the course of the experiments came from three separate batches, but is assumed to be uniform in composition. The thickness of developed samples from two of the batches was measured with a profilometer and found to be seven microns.

3.2 Film Preparation and Processing

Polaroid's DMP-128 requires activation by absorption of water before exposure and development [7]. This is achieved in a reproducible manner by exposing the emulsion (which has been stored in a very low humidity environment) to a controlled-humidity atmosphere for a prescribed time period. The necessary time interval depends on the ambient humidity and on the thickness of the material. The humidity is controlled using a saturated salt solution of calcium nitrate in a closed container. At equilibrium, the relative humidity above this solution is 51.0%; this remains fairly constant over a moderate temperature range around room temperature. In order to insure equilibrium conditions inside the chamber, the solution is constantly stirred with a magnetic bar and the air is circulated in a closed loop above the solution. For optimum activation under these conditions, the seven micron emulsion is incubated

for four minutes. In order to prevent evaporation or absorption of more water into the emulsion after activation in the chamber is complete, the laboratory air is also maintained at a relative humidity of 51 ± 5% and the xylene, which is hydrophilic, is water-saturated.

After activation, the film is placed in the holder with the emulsion side to the prism and time is allowed for all vibrations and air currents to cease. After exposure, the film is illuminated with white light for two minutes to polymerize any remaining monomer and fix the monomer gradient in the material. The light source is a 60 W tungsten bulb in a reflector held 8" from the film. To insure repeatability in case of any post-exposure monomer diffusion, a ten-second delay is counted after exposure before the film is illuminated. Next, the film is placed in the processing fluid for two minutes and then rinsed liberally with isopropanol or methanol. Afterwards the film is dried in the vapors of boiling isopropanol for one minute.

3.3 Measurements

3.3.1 Spectral transmission of the system

Because the emulsion is coated on a glass substrate, the properties of the substrate must be taken into account in determining the efficiency of the processed hologram. Also of interest is the transmission characteristic of the polymer which has been flooded and developed, but which has not been modulated by an interference pattern. A spectrophotometer plot of the glass substrate and of the exposed photopolymer on the substrate is shown in figure 3.2. The glass substrate begins to absorb the light around a wavelength of 360 nm and begins absorbing strongly at 320 nm. The photopolymer begins absorbing at 500 nm and absorbs at wavelengths lower than 400 nm. This can be considered a baseline value for the scattering of light by the polymer. In the spectral range used in this work, the absorption can be neglected.

3.3.2 Diffraction efficiency

All irradiance measurements were made with a Jodon light intensity meter held

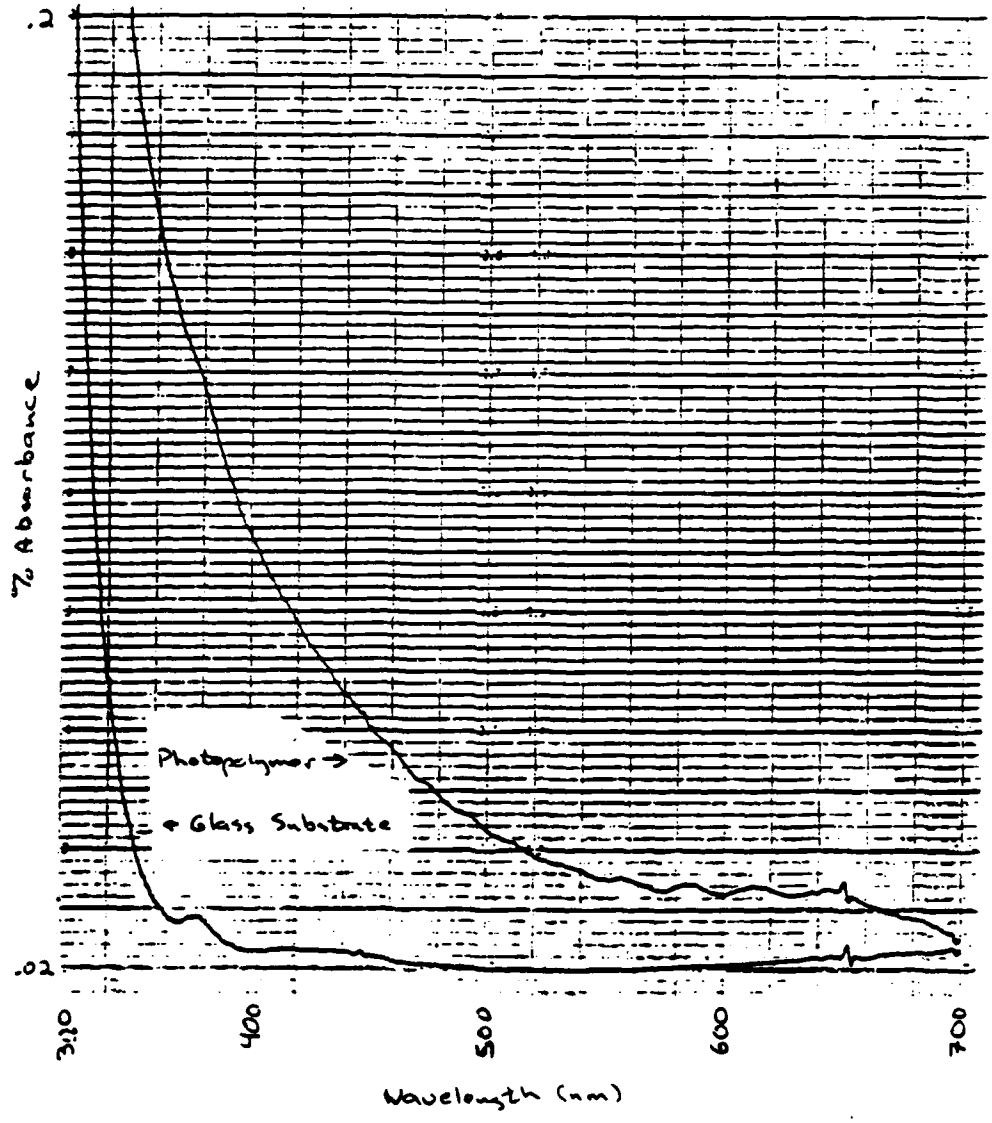

Figure 3-2. *Spectral transmission for the glass substrate and for the exposed polymer on the glass substrate.*

perpendicular to the beam. Measurements of the diffraction efficiency were made by illuminating a 1 mm diameter circle in the center of the hologram. In order to account for Fresnel reflection at the surface of the glass and possible absorption by the polymer, the beam passing through a portion of the exposed polymer in which no hologram is recorded was measured and considered to be the incident irradiance; all diffraction efficiency calculations are made relative to this. In order to measure the angular sensitivity of the hologram, the film plate was rotated through from 30 to 50 degrees around the constructing reference angle while

measuring the light diffracted into the first order.

The wavelength sensitivity measurements* were performed using four different lasers with different wavelengths. The diffraction efficiency was optimized for the 514.5 nm wavelength and all other measurements were normalized relative to this value. The other wavelengths used were 442, 488 and 632.8 nm. All measurements were made at the same incident angle. It must be borne in mind that this is only an approximate measurement.

Another important concern is the type of mechanism responsible for the diffraction of the incident beam--an index of refraction gradient or surface relief. If no thickness variation is found, then the hologram may be assumed to be a volume hologram. A common method to test for surface relief in holograms is to gate the hologram with a liquid of approximately the same index of refraction; this is known as index-matching. The liquid fills in any thickness variations and negates any effect of surface relief by eliminating any difference in optical path length. This was done with xylene and glycerin (n = 1.5). The hologram surface (including one coated with 150 Angstroms of gold in a vacuum evaporation chamber) was also inspected with a metallurgical microscope and a scanning electron microscope.

3.4 Data and Analysis

3.4.1 Diffraction efficiency

The diffraction efficiency of a holographic material depends on a number of variables: the exposure energy, grating period, material thickness and visibility can all be tailored to suit one's needs. In manufacturing holographic optical elements, maximum diffraction efficiency is (usually) desired; in making display holograms, linearity is important. The $\sqrt{\eta}$ vs. E_0 and V plots proposed by Lin [11] provide much of the necessary information.

---

* The wavelength sensitivity measurements were graciously performed by Tom Stone of the University of Rochester Optics Department.

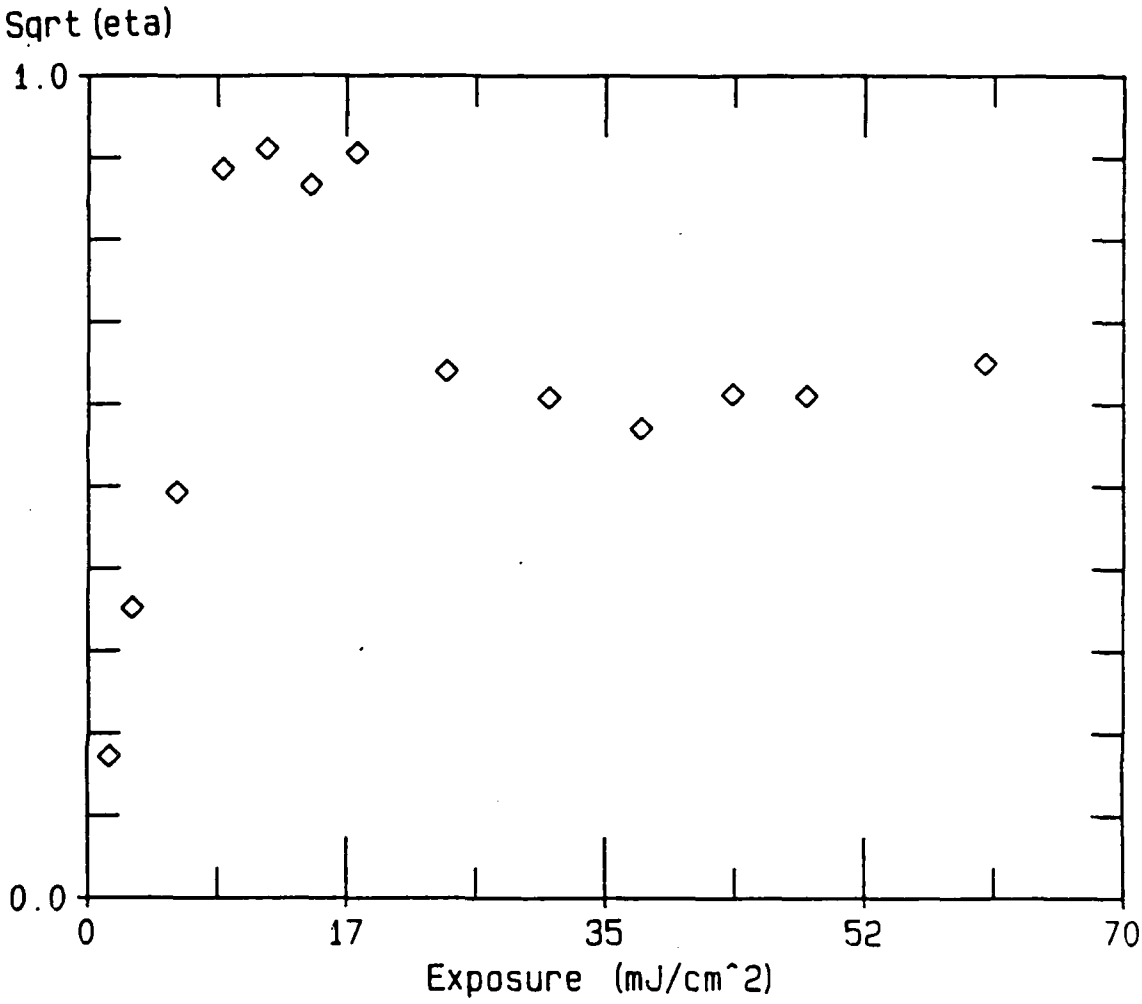

Figure 3-3. $\sqrt{\eta}$ **vs.** E_0 **for** $\theta_R = 0$ **and** $\theta_O = 30$. $V = .97$.

Shown in figure 3-3 is the plot of $\sqrt{\eta}$ vs. E_0 for $\theta_R = 0$ and $\theta_O = 30$ for a constant value of $V = 0.97$. The diffraction efficiency rises quickly with exposure to a maximum around 14 mJ/cm^2. The efficiency decreases again to roughly two-thirds the maximum efficiency at twice the exposure. It remains fairly constant thereafter, rising again slightly for very high exposure energies. The initial rise to high efficiency is approximately linear, indicating that the sensitivity is not strongly dependent on the exposure in that regime. The diffraction efficiency is high, reaching a peak of 82.9%. According to Kogelnik's coupled wave theory, the efficiency should

peak and fall again to zero. This is not observed and there are a couple of possibilities for this. Kogelnik's theory holds well only for holograms with high values of Q. The Q-factor for this set of holograms is 28.5. While this value is greater than ten, which is quoted by Kogelnik as the region in which the coupled wave theory holds, the cycling of the efficiency from zero to one as the index of modulation increases is not always observed to happen unless Q is very large [12]. Another possibility is that of surface relief in addition to the volume effects. While volume and plane holograms are theoretically distinct, the dividing line between them is blurred and most holograms show some effects of both types. This is reinforced by the observation of fringes in all of the holograms using the metallurgical microscope.

The plot of $\sqrt{\eta}$ for $\theta_R = \theta_O = 16$ shown in figure 3-4 is very similar to the previous plot. The efficiency reaches a peak of 90.0% for an exposure energy of 6.7 mJ/cm^2 and decreases to an efficiency of around 50% at twice the exposure. The diffraction efficiency appears to rise to a second peak near $E_0 = 20$ mJ/cm^2. The index of modulation of the hologram with exposure energy of 16.7 mJ/cm^2 can be calculated to be .061.

Figure 3-5 shows a plot of $\sqrt{\eta}$ vs. E_0 for $\theta_R = 0$ and $\theta_O = 9$ and constant values of visibility. For V = .99, the diffraction efficiency rises quickly to an apparent peak near 16 mJ/cm^2 and then decreases much like the aforementioned examples. In agreement with Lin [10], the diffraction efficiency for V = .85 rises more slowly than that for V = .99. The slope is approximately linear, although not completely. Again, the peak efficiency is followed by a drop and then a slow rise. The diffraction efficiency for V = .32 rises slowly, but quite steadily, only reaching a peak of less than 50% for an exposure of 50 mJ/cm^2 before leveling off.

The other plot proposed by Lin [11] is a plot of $\sqrt{\eta}$ vs. V for constant E_0. An example of this is shown in figure 3-6 for $\theta_R = \theta_O = 16$ and $E_0 = 5.0$. The plot is almost linear, showing only small dependence on visibility. For a hologram with a relatively uniform exposure intensity, one can see the limits of linear recording from this plot. Many holograms, such as

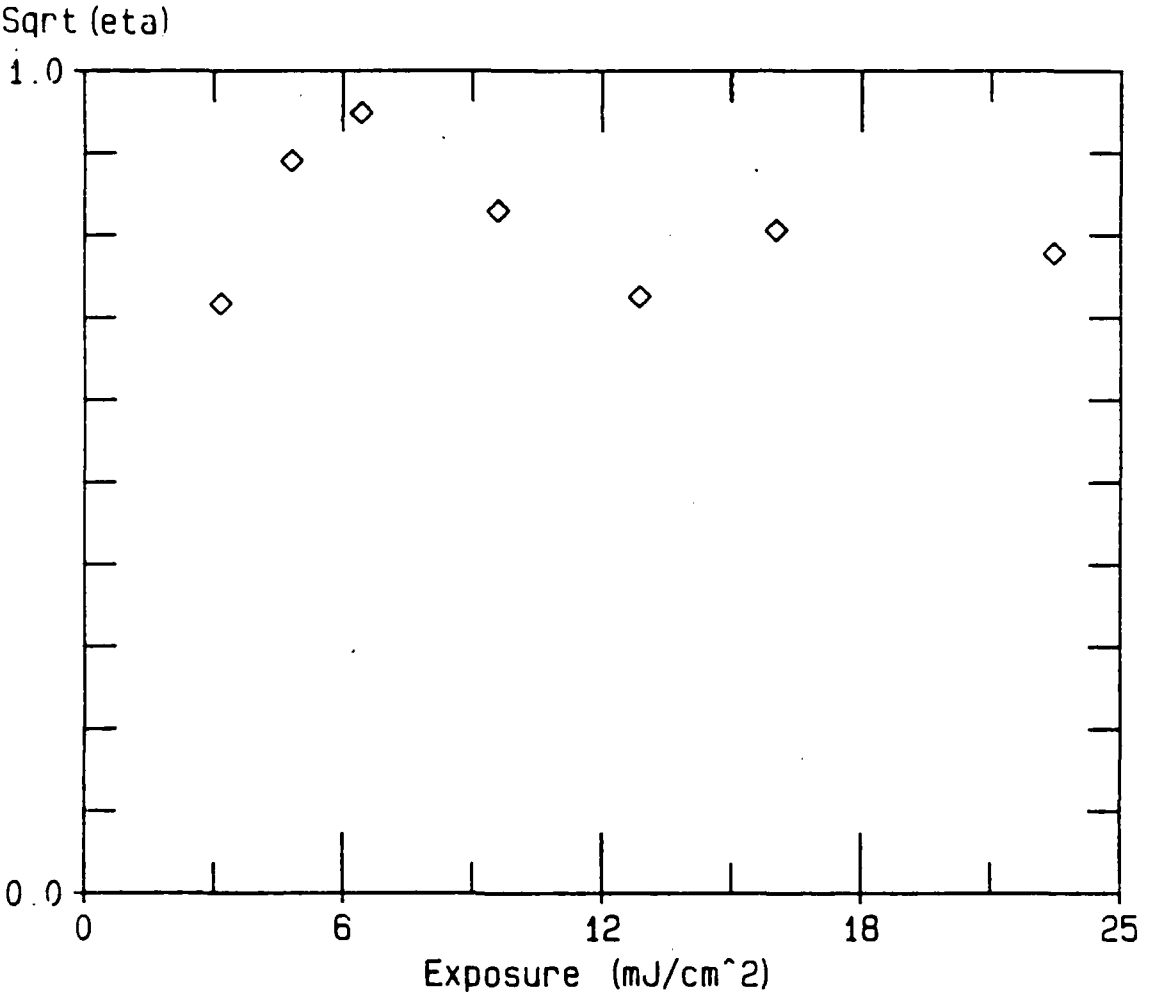

Figure 3-4. $\sqrt{\eta}$ **vs.** E_0 **for** $\theta_R = \theta_O = 16$. $V = 1.0$.

diffusely-lit object holograms are fairly uniform in exposure, but not in visibility. For holographic optical elements such as diffraction gratings, the visibility is constant and the plots of $\sqrt{\eta}$ vs. E_0 are more revealing.

Several approaches were tried to resolve the question of the mechanism of diffraction. Index-matching produced inconclusive results. When index-matching using xylene, the diffraction efficiency decreased from 61.2% to 1.7% on one hologram made with a total

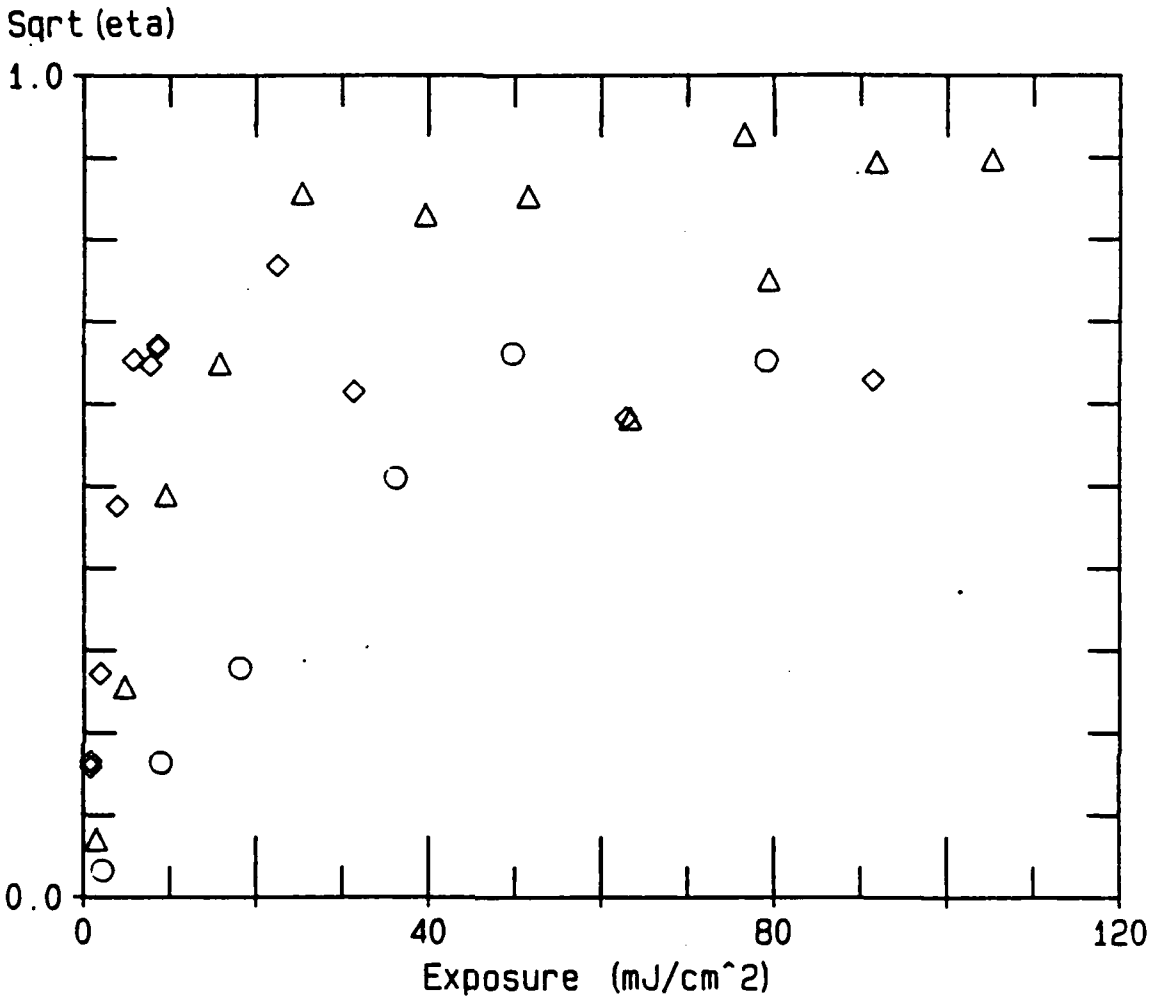

Figure 3-5. $\sqrt{\eta}$ **vs.** E_0 **for** $\theta_R = 0$ **and** $\theta_O = 9$. $V_\Diamond = .99$, $V_\Delta = .85$, $V_O = .32$

interbeam angle of 30 degrees (d = .80 μm). This can not be due completely to negating any surface relief as the maximum diffraction efficiency of such holograms is 33.9%. The hologram also disappears when wetted with methanol or isopropanol and returns to the original diffraction efficiency after drying. These liquids (with low surface tensions) may be filling in tiny cracks or voids in the polymer which account for the change in index of refraction. This method of hologram formation in phase gratings was proposed by Curran and Shankoff [8] for dichromated gelatin and could also be present in the photopolymer. Index-matching was also performed

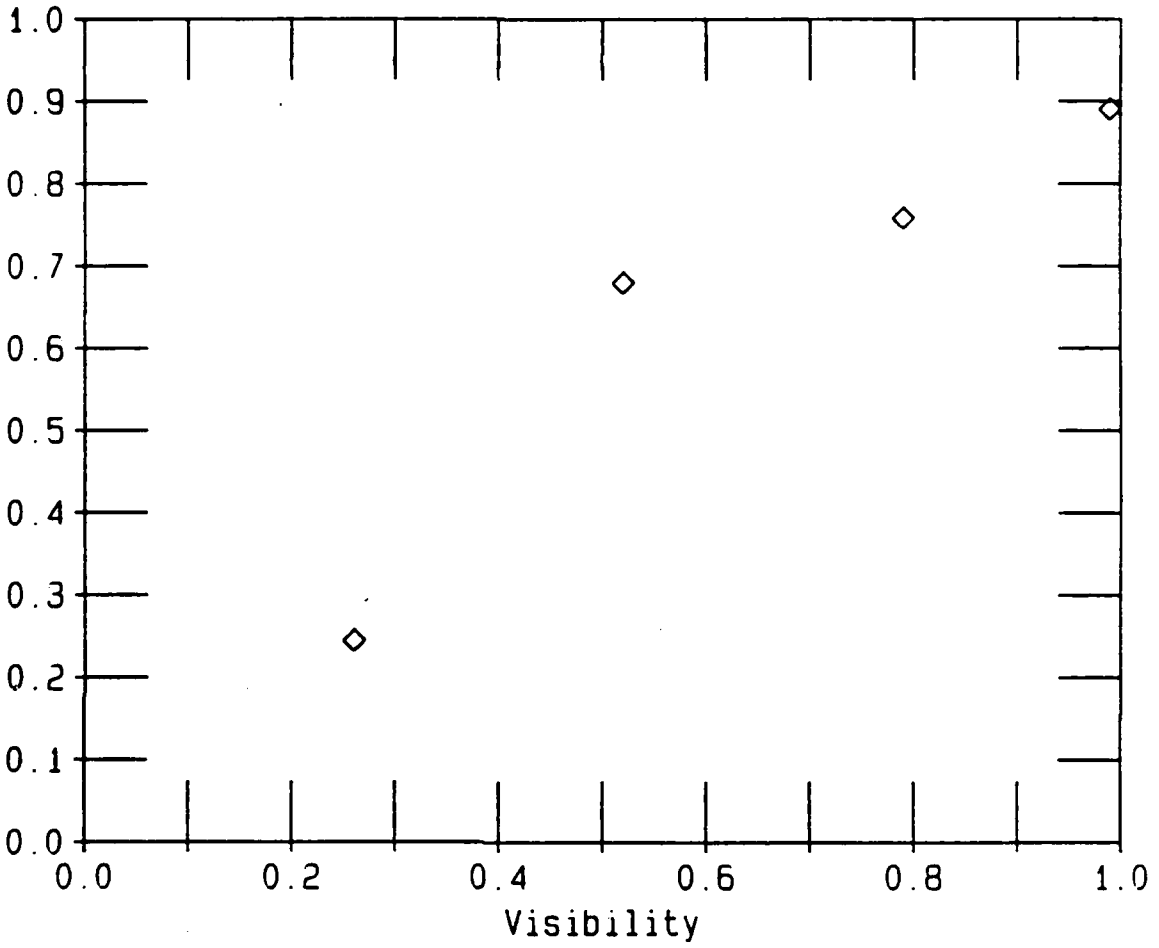

Figure 3-6. $\sqrt{\eta}$ **vs. V for** $\theta_R = \theta_O = 16.$ $E_0 = 5.0.$

using glycerin (n = 1.5), a more viscous liquid. The observed diffraction efficiency of the same hologram decreased to 6.6% upon application of the glycerin. Assuming that the glycerine does not penetrate the hologram as easily as do the alcohols and xylene, the smaller drop in diffraction efficiency could be attributed to not filling in all or as many of the voids. Shankoff noted that in dichromated gelatin the emulsion had pulled away from the substrate, creating voids between the substrate and the emulsion. This could account for the higher diffraction efficiency when gated with glycerin rather than xylene--having a higher surface tension, the

Figure 3-7. Photograph of surface relief in hologram with $\theta_R = 0$ and $\theta_O = 9$. Magnified 700 times.

glycerin could not flow as well as the xylene and fill deep voids. A second hologram, with a total interbeam angle of 9 degrees, originally had a diffraction efficiency of 71%, but fell to 12% when gated with glycerin and 4.5% when gated with xylene. The holograms were also observed under a metallurgical microscope for possible thickness variations. Surface modulation was visible in all the holograms, even the holograms with smaller periods. The relief was not measurable, but appears to be less than one micron. Small scale surface roughness was also visible in all holograms. A photograph of a hologram which was coated with a 15 nm layer of gold in a vacuum evaporator is shown in figure 3-7. The period was measured to be 2.4 μm which corresponds to the calculated value for the incident angles of $\theta_R = 0$ and $\theta_O = 9$. The same hologram was viewed in a scanning electron microscope. The electron beam was visibly destructive to the hologram and no surface relief could be seen, although surface roughness and irregularities were visible at magnifications from 500 to 20000 times.

3.4.2 Angular and wavelength sensitivity

Angular sensitivity measurements were made on four sets of slides with different incident angles: $\theta_R = 0$ and $\theta_O = 9$, $\theta_R = 0$ and $\theta_O = 12$, $\theta_R = 0$ and $\theta_O = 30$ and $\theta_R = \theta_O = 16$.

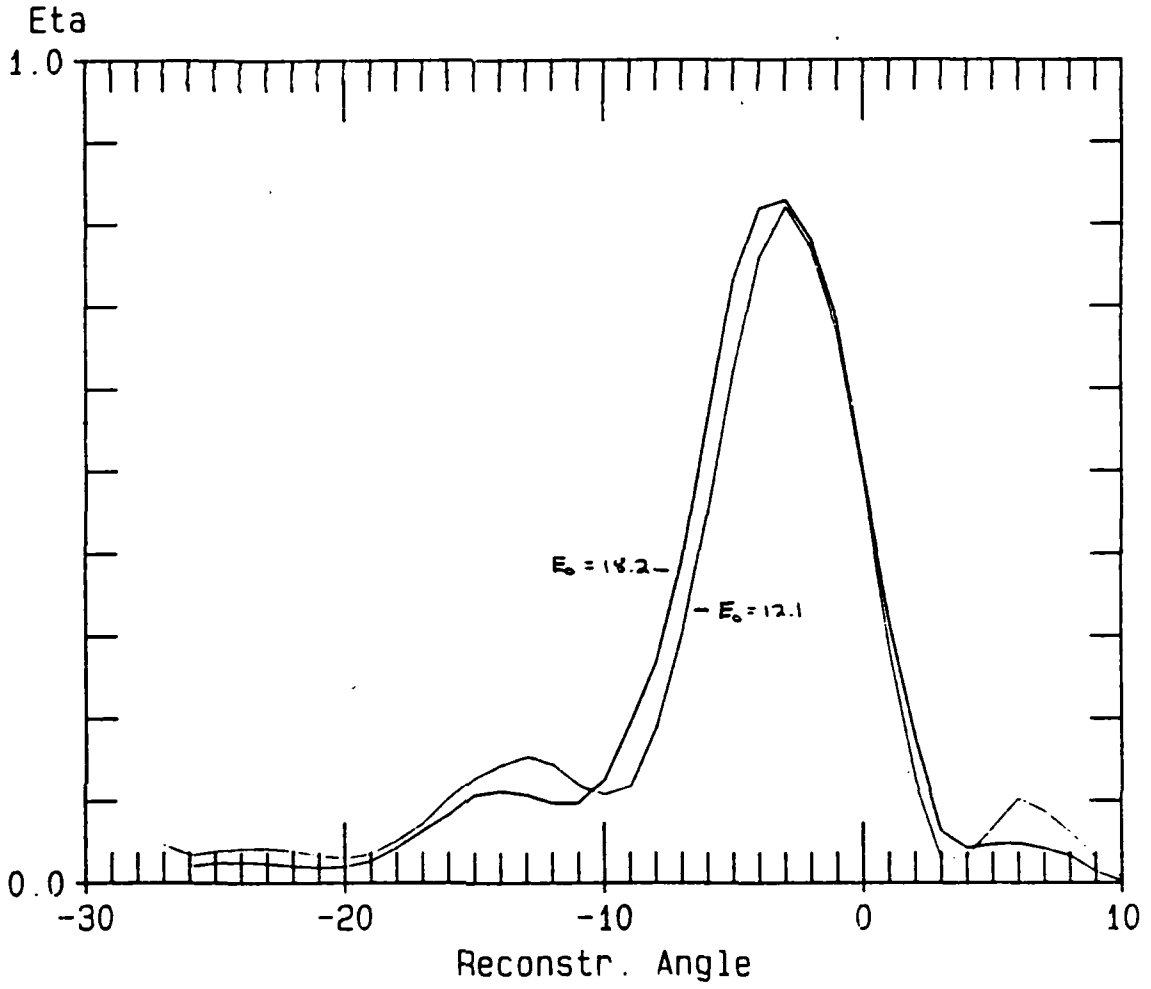

Figure 3-8. Angular sensitivity measurements for $\theta_R = 0$ and $\theta_O = 30$. $E_0 = 12.1, 18.2$.

Shown is figure 3-8 are two measurements for $\theta_R = 0$ and $\theta_O = 30$. For increasing index of modulation, the side lobes are seen to increase as predicted by Kogelnik [4]. The half-power bandwidth is 8 degrees for both; it should show no change for increasing efficiency and does not. The calculated half-power bandwidth from Eq. 2.38a is 6.5 degrees. For the plot shown in figure 3-9, the calculated half-power bandwidth is 19.6 degrees; when measured, it is 22 degrees. From these two plots, it can easily be seen that the angular sensitivity becomes much smaller for greater angles of incidence.

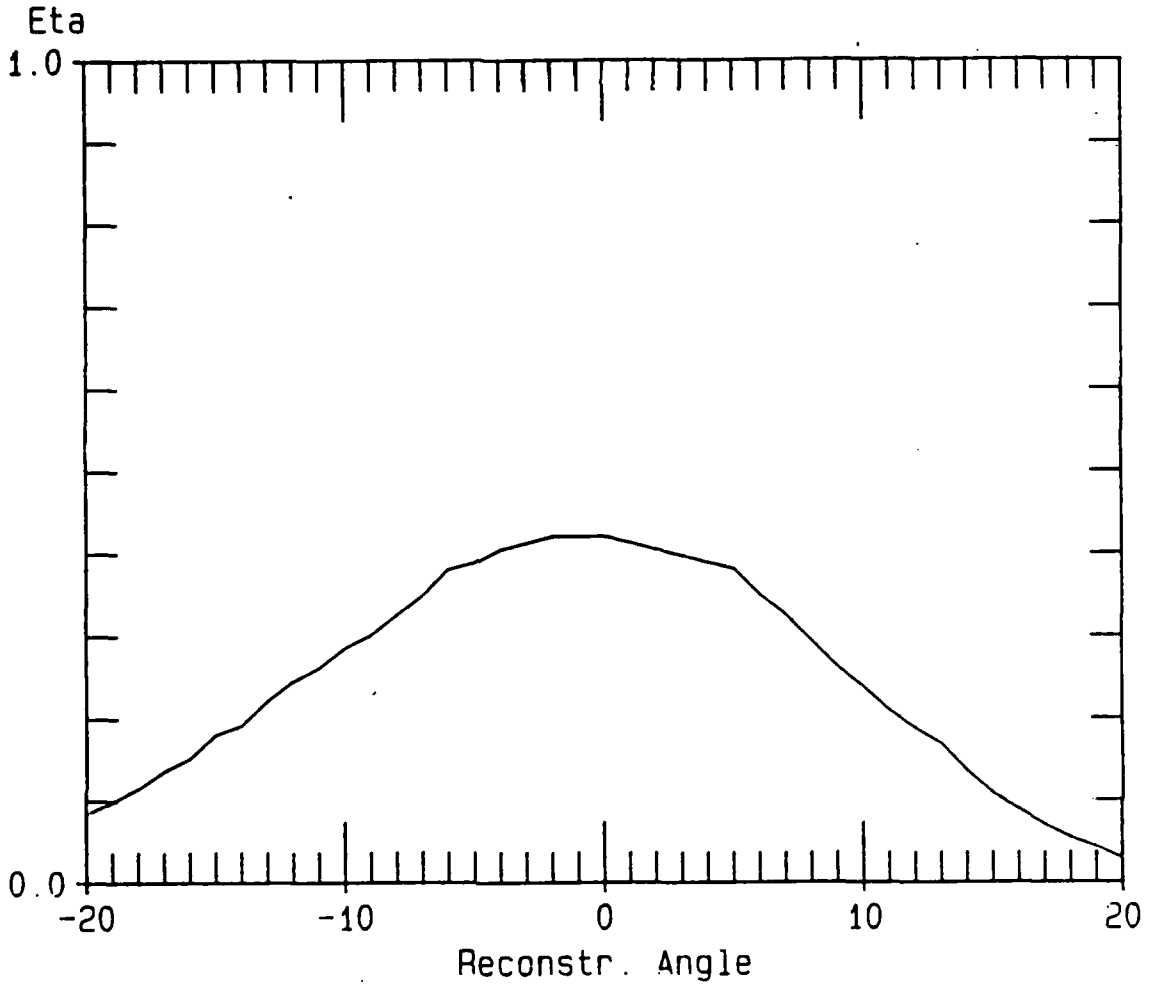

Figure 3-9. Angular sensitivity measurements for $\theta_R = 0$ and $\theta_O = 9$. $E_0 = 15.8$.

A progression of plots shown in figure 3-10 presents quite clearly the increasing efficiency of the side lobes as the index of modulation increases. The exposure energies vary from 3.3 to 23.4 mJ/cm^2, while the index of modulation varies from .02 to greater than .06. While the efficiency of the center lobe increases and decreases as expected, though to a lesser degree than Kogelnik's theory predicts, the half-power bandwidth remains the same. The calculated value is 6.1 degrees and the measured value is approximately 8 degrees.

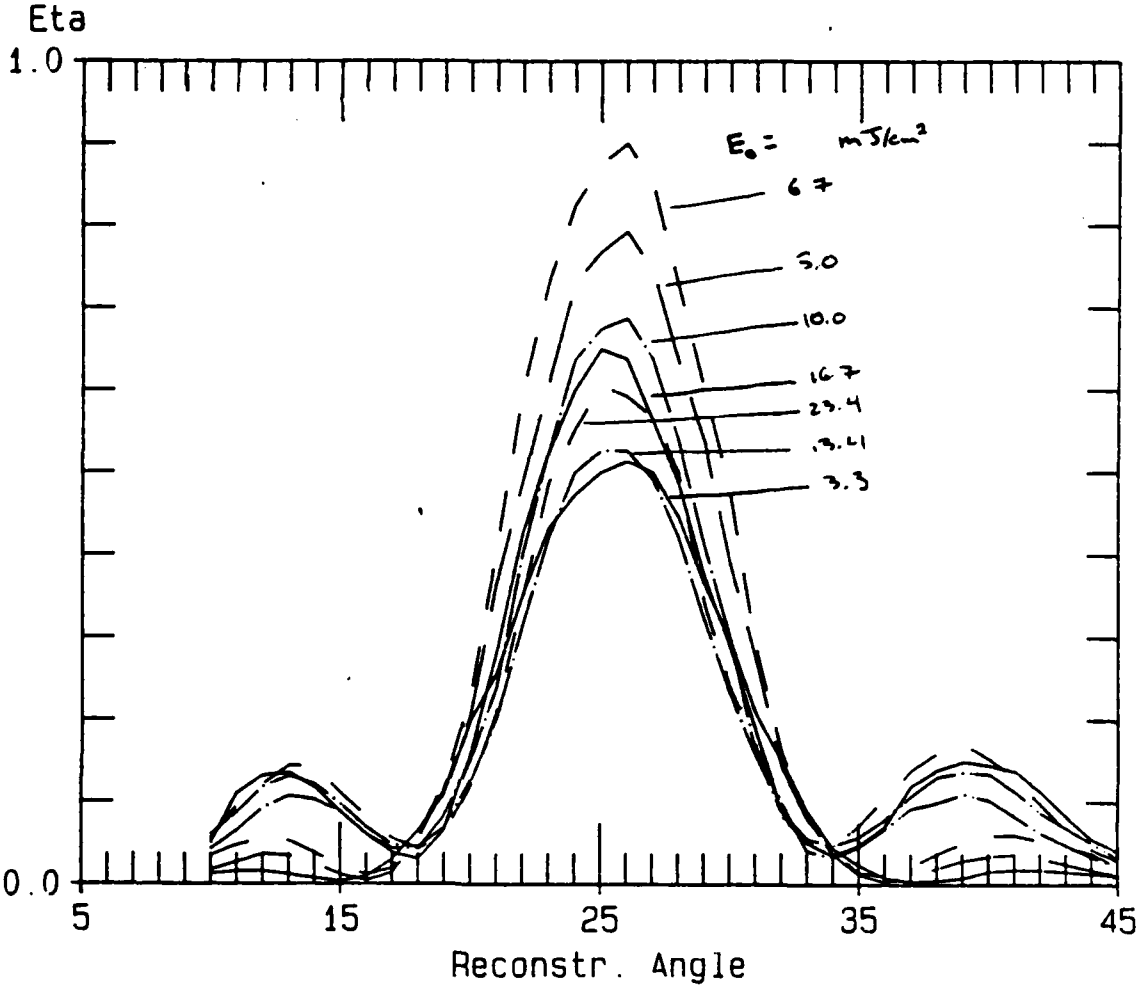

Figure 3-10. Angular sensitivity measurements for $\theta_R = \theta_O = 16$. $E_0 = 15.8$.

The wavelength sensitivity was measured for a hologram with incident angles of $\theta_R = \theta_O = 16$. The diffraction efficiency was peaked at 21.2 degrees for the green 514.5 nm light and then was measured for that same angle with wavelengths of 442.0, 488.0 and 632.8 nm. The result is shown in figure 3-11. The half-power bandwidth is measured to be approximately 180 nm; the calculated value is 142 nm. The experiment itself was not very exact and Kogelnik's theory is also approximate, so the correlation is acceptable.

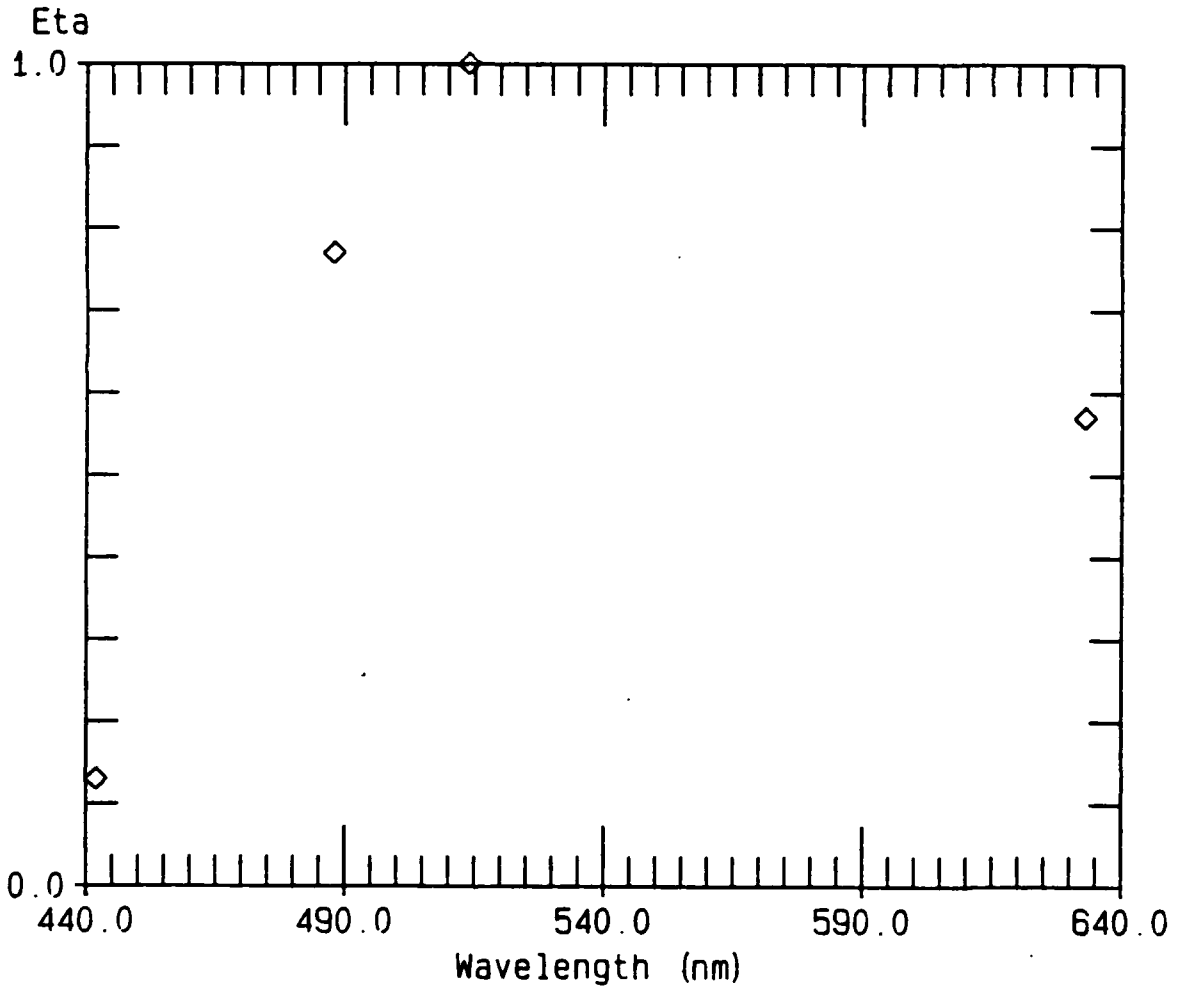

Figure 3-11. Wavelength sensitivity measurement--η vs λ.

3.4.3 Shrinkage

At different stages in processing, the thickness of DMP-128 changes. During activation the emulsion absorbs water and increases in thickness. As the exposure is made with the emulsion in this state, the thickness T at this point is the thickness for hologram formation. The measured thickness after processing is seven microns. Not being able to measure the thickness during exposure, it must be calculated from the theory in Chapter 2. Solving Eqs. 2.48a & b

for an angle of 9 degrees, the shrinkage factor s is seen to be .82. This translates to a shrinkage of about 18%. As a rough confirmation of this shrinkage factor, reflection holograms recorded in the red "play back" in the green-blue region. In reflection holograms the fringe planes are parallel to the substrate, so the period changes directly with the thickness. A spectrophotometer measurement of the absorption by an in-line reflection hologram constructed with the 632.8 nm line of a He-Ne laser showed a peak absorption around 480 nm, so a rough estimate of the shrinkage factor is s = 480/632.8 = .76. Since the object signal was not a plane wave in this case, this result must be regarded as a rough estimate only.

3.4.4 Resolution

The resolution requirements for phase transmission holograms constructed with a wavelength of 632.8 nm range from 0 cycles/mm (for an inter-beam angle of zero degrees) to 3160 cycles/mm (for an inter-beam angle of 180 degrees). The range of resolutions used in this study extended only from 410.4 to 1335.6 cycles/mm. These spatial frequencies were well within the resolution capabilities of DMP-128.

3.4.5 Handling and processing

DMP-128 is an extremely easy film to use. The film can be stored for up to a year at a relative humidity less than about 35%. Some of the film used in this experiment was 6 months old at the time of exposure; a maximum diffraction efficiency of 90% was achieved with one of these plates. With the exception of silver halide, most other films have a shelf life of days or hours, not months, once they are formulated or coated on a substrate. After flooding with light, DMP-128 can be developed and fixed with one chemical bath and then dried. Some films, one of which is the Dupont photopolymer, can develop themselves with no processing and thus produce near real-time holograms, but they require fixing in order to prevent the hologram from degrading in a matter of hours or days. DMP-128 must be fixed and developed chemically, but the whole process requires only five to six minutes and the holograms show little sign of

degrading, even under conditions of high humidity. Another advantage of DMP-128 is the option of using safelights during all stages of exposure and processing. In the case of red-sensitized film, the laboratory may be illuminated with blue safe-lights even after the emulsion is activated.

The activation of the film in a controlled humidity chamber must be determined experimentally, but once the optimal activation time has been found the incubation period need only be held constant; the film can be very activated in an easily reproducible manner. In order to prevent the loss or additional absorption of water after activation, the laboratory must be maintained at a relative humidity near 51%. The shrinkage discussed above is a disadvantage, but with additional processing baths, this can be at least partially corrected. DMP-128 has been observed to crack along the fringe planes when overexposed or subjected to repeated drying. This is a result of stressing the material too much and can generally be avoided.

Chapter 4. CONCLUSIONS

In this thesis a new holographic recording system was tested. Polaroid's DMP-128 film is a photopolymer medium which produces phase holograms. The phase change is caused by the polymerization of monomers by photo-initiation. A hologram with a diffraction efficiency of 90% was produced. An index of modulation in excess of .06 was achieved for high exposure energy without harming the integrity of the emulsion. Regions of linearity for $\sqrt{\eta}$ plotted against visibility and exposure were shown. The mechanisms responsible for diffraction by the photopolymer were investigated; both surface relief and volume phase modulation are observed to be present. Wavelength and angular sensitivity were measured and found to agree closely with Kogelnik's coupled wave theory. Resolution and the extreme ease of handling and processing of DMP-128 were also discussed.

4.1 Suggestions for Further Research

All of the holograms fabricated in the process of this research were formed with λ = 632.8 nm. The emulsion, however, is sensitive over a broader range of wavelengths than this. Others have obtained an estimate for the spectral sensitivity of DMP-128 [12], but a rigorous experiment has yet to be conducted to verify this. To accomplish this, holograms should be constructed at a given intensity for a range of wavelengths and then be measured for diffraction efficiency. Additional investigation could be directed toward a similar characterization of the blue- and green-sensitized formulations of DMP-128. The more complicated problem of reflection holography can also be explored much like transmission has been in this work.

The major thrust of any additional work should be centered around the processing of the film. Variables such as effects of flooding time and delay time before flooding need to be measured to check for diffusion of the monomer. The intensity and duration of the flood also merits investigation. The chemical processing could be tested. Variations in the chemical

components should be tried and their effects noted. Closely linked with this would be an investigation into methods to swell the emulsion back to its thickness during exposure.

References

[1] Smith, H. M., *Principles of Holography, 2nd ed.*, John Wiley & Sons, New York, 1975.

[2] Smith, H. M., ed., *Holographic Recording Materials*, Springer-Verlag, Berlin, 1977.

[3] Collier, Robert J., et al., *Optical Holography*, Academic Press, Inc., Orlando, 1971.

[4] Kogelnik, H., "Coupled Wave Theory for Thick Hologram Gratings", Bell System Technical Journal, 48:9, Nov. 1969, pp. 2909-2947.

[5] Guenther. B. D., to be published.

[6] Rick Feinberg, "An Interview with Richard T. Ingwall: Photopolymers for Holography." Optical Engineering Reports, No. 31, July 1986, pp. 1, 4.

[7] R.T. Ingwall, A. Stuck, W.T. Vetterling, "Diffraction Properties of Holograms Recorded in DMP-128", Polaroid technical report no. 615-05.

[8] Curran, R. K. and Shankoff, T. A., "The Mechanism of Hologram Formation in Dichromated Gelatin", Applied Optics 9, No. 7, July 1970, pp. 1651-7.

[9] Ingwall, R. T. and Fielding, H. L., "Hologram Recording with a New Polaroid Photopolymer Recording System", SPIE Vol. 523 Applications of Holography (1985), pp. 306-12.

[10] Vilkomerson, D. H. R. and D. Bostwick, D., "Some Effects of Emulsion Shrinkage on a Hologram's Image Space", Applied Optics 6, No. 7, July 1967, pp. 1270-1.

[11] Lin, L. H., "Method of Characterizing Hologram-Recording Materials", Journal of the Optical Society of America, Vol. 61, No. 2, February 1971, pp. 203-8.

[12] Stone, Thomas, personal communication.

[13] Norton, M. C., "Holographic Applications of Polaroid DMP-128", no published date.

END

11-86

DTIC